Supporting information

A Synergistic Catalysis of Imidazole Acetate Ionic Liquids for Methanolysis of Spiral Poly (ethylene 2,5-furandicarboxylate) under a Mild Condition

Xiaoling Qu,[a, b] Guangyuan Zhou,[b] Rui Wang,[b] Bolei Yuan,[a] Min Jiang*[b] and Jun Tang*[a]

Characterization of the IL catalysts

Series of tetrabutylphosphonium-based ILs were synthesized, and their structures were determined by ^{1}H NMR, ^{13}C NMR, and ^{31}P NMR. All the detailed characterization results are provided in Fig. S1–S22. The obtained spectra were in good accordance with the intended chemical structures. Taking ^{1}H NMR spectrum of [P_{4444}][LAc] for example (Fig. S1), the signals at δ 1.22-1.21 ppm and 4.01-3.96 ppm could be attributed to H-a and H-b of the [$CH_3CHOHCOO$]$^-$ anion. The chemical shifts of H-c, H-d, H-e and H-f in tetrabutylphosphonium cation were observed at δ 2.08-2.02 ppm, 1.48-1.31 ppm, and 0.83-0.80 ppm respectively. The thermal stability of the synthesized ILs was checked by thermogravimetric analysis (TGA), as shown in Fig. S25, and all of tetrabutylphosphonium-based ILs exhibited excellent thermal stability (T_d 290-335 °C).

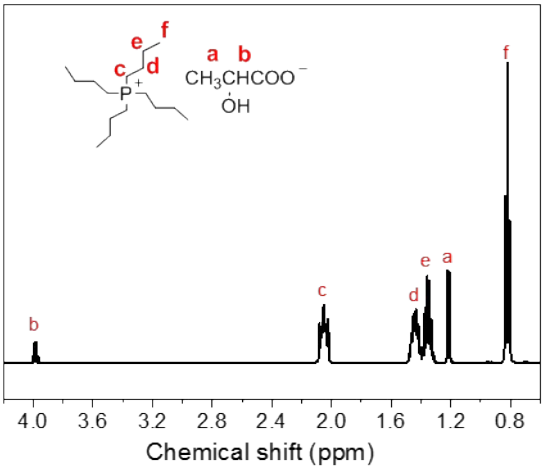

Fig. S1 ^{1}H NMR of P-LAc

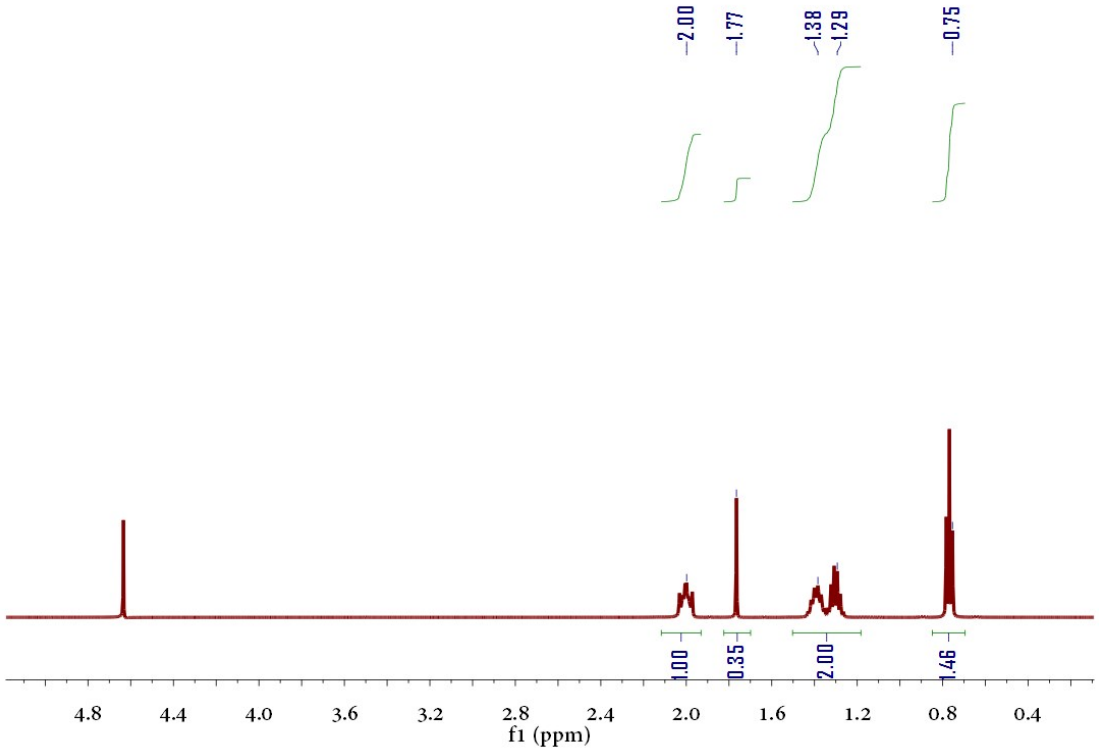

Fig. S2 The ^{1}H NMR spectrum of $[P_{4444}][OAc]$ (D_2O).

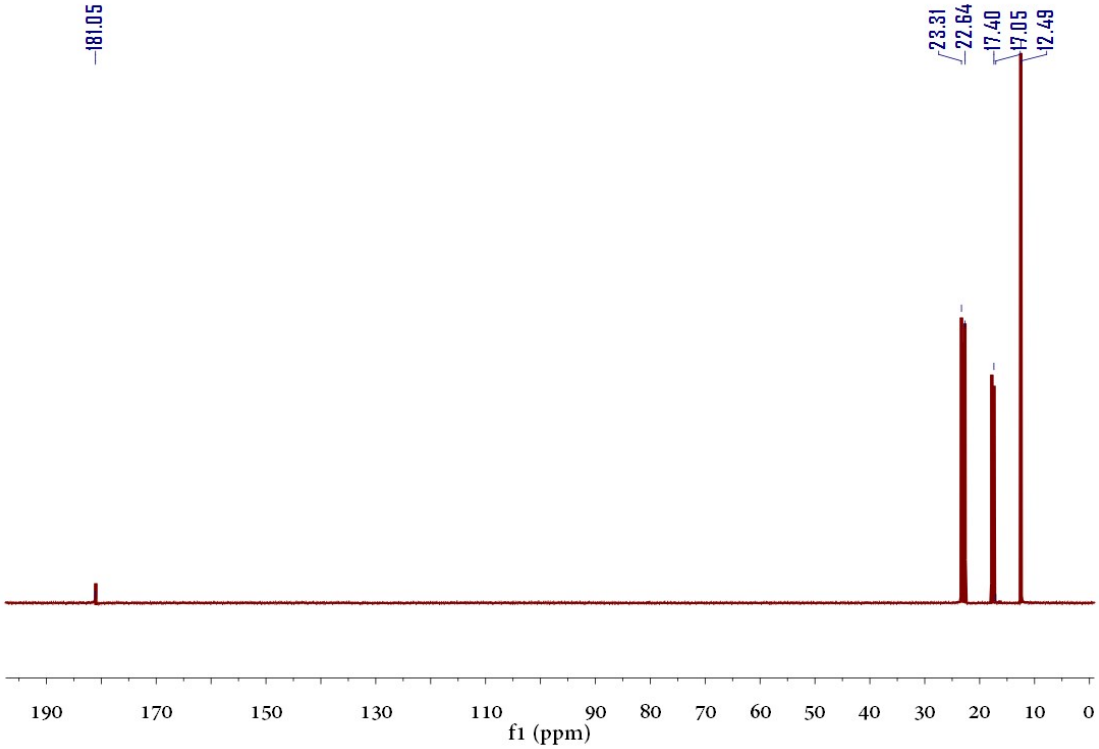

Fig. S3 The ^{13}C NMR spectrum of $[P_{4444}][OAc]$ (D_2O).

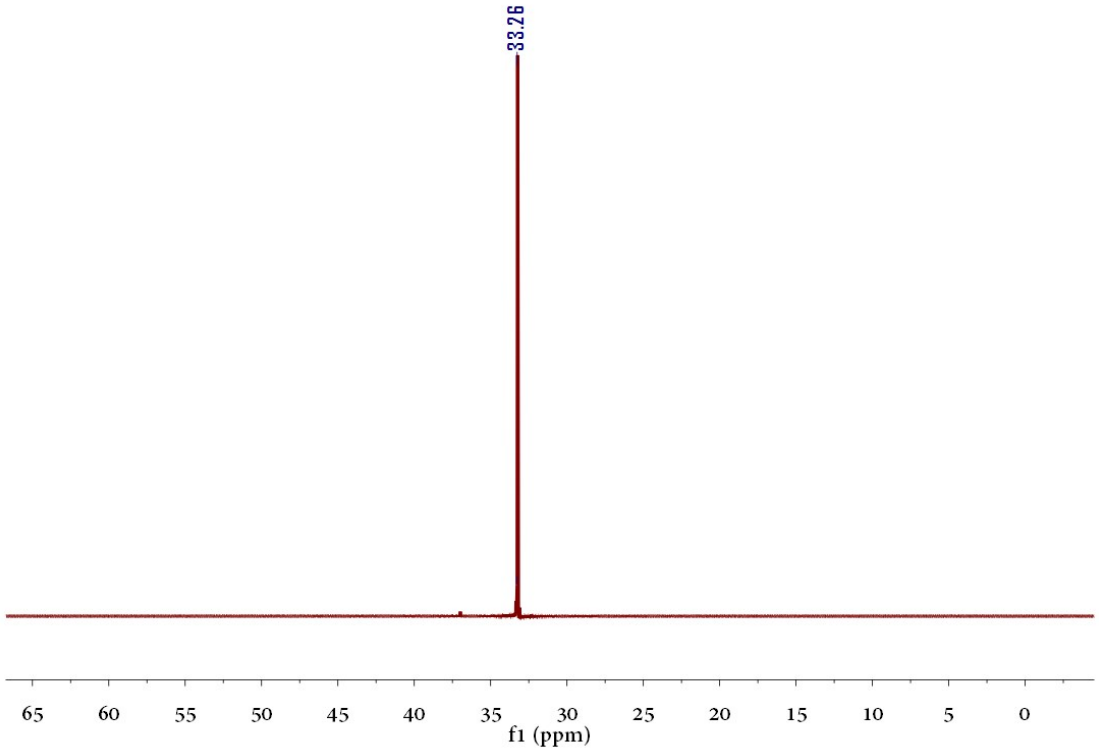

Fig. S4 The ^{31}P NMR spectrum of $[P_{4444}][OAc]$ (D_2O).

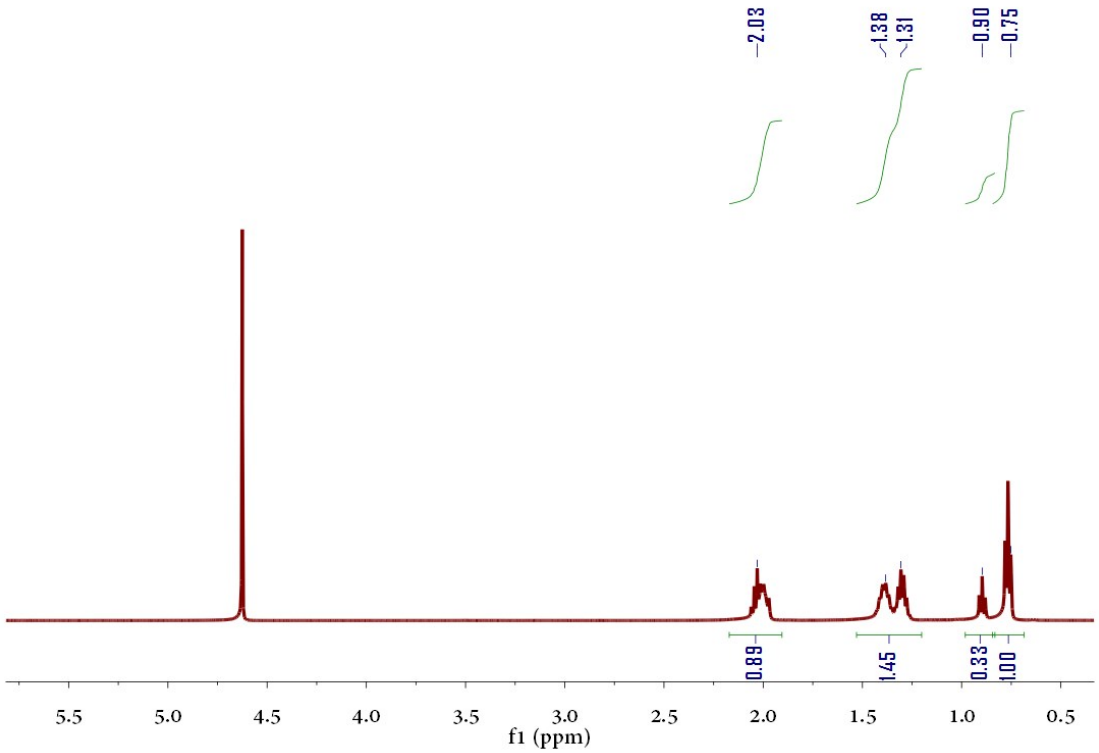

Fig. S5 The ^{1}H NMR spectrum of $[P_{4444}][PAc]$ (D_2O)

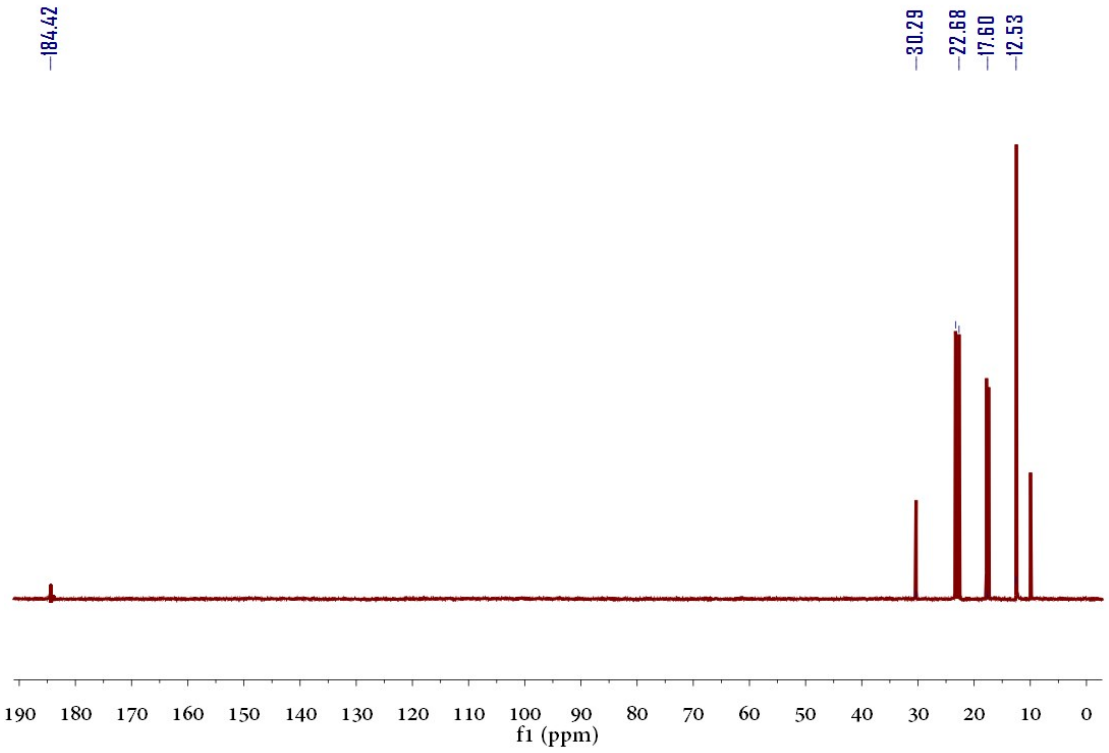

Fig. S6 The ^{13}C NMR spectrum of $[P_{4444}][PAc]$ (D_2O).

Fig. S7 The ^{31}P NMR spectrum of $[P_{4444}][PAc]$ (D_2O).

.

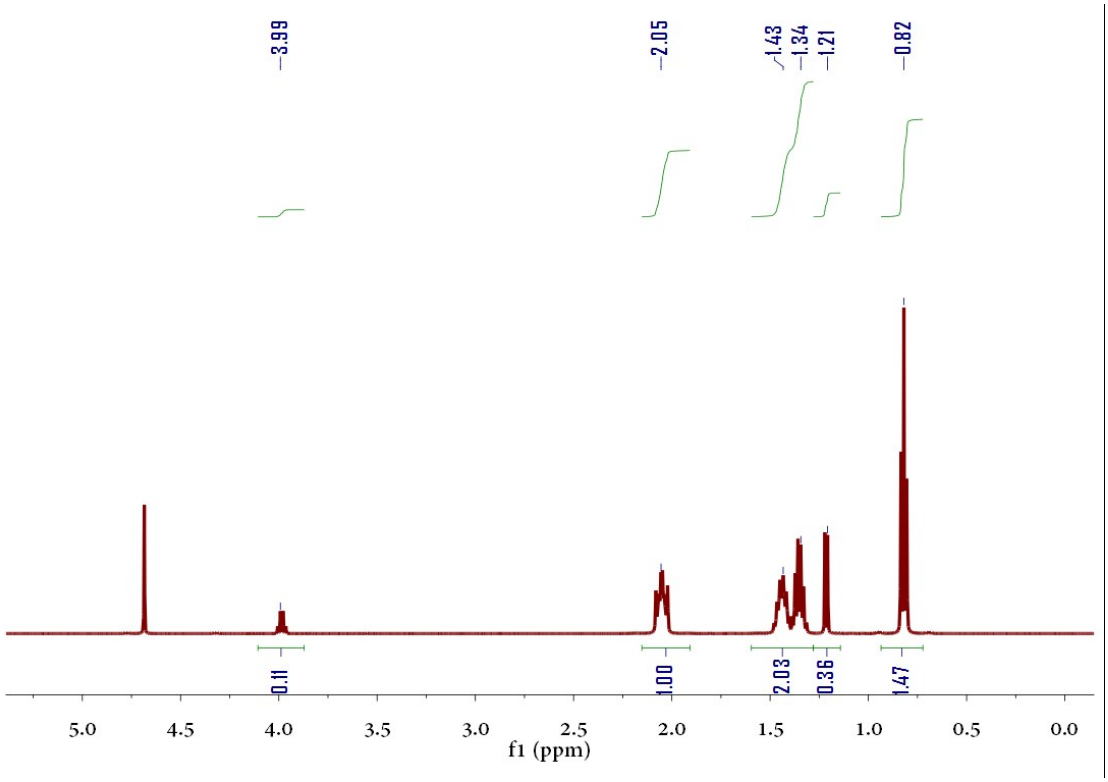

Fig. S8 The ^{1}H NMR spectrum of $[P_{4444}][LAc]$ (D_2O).

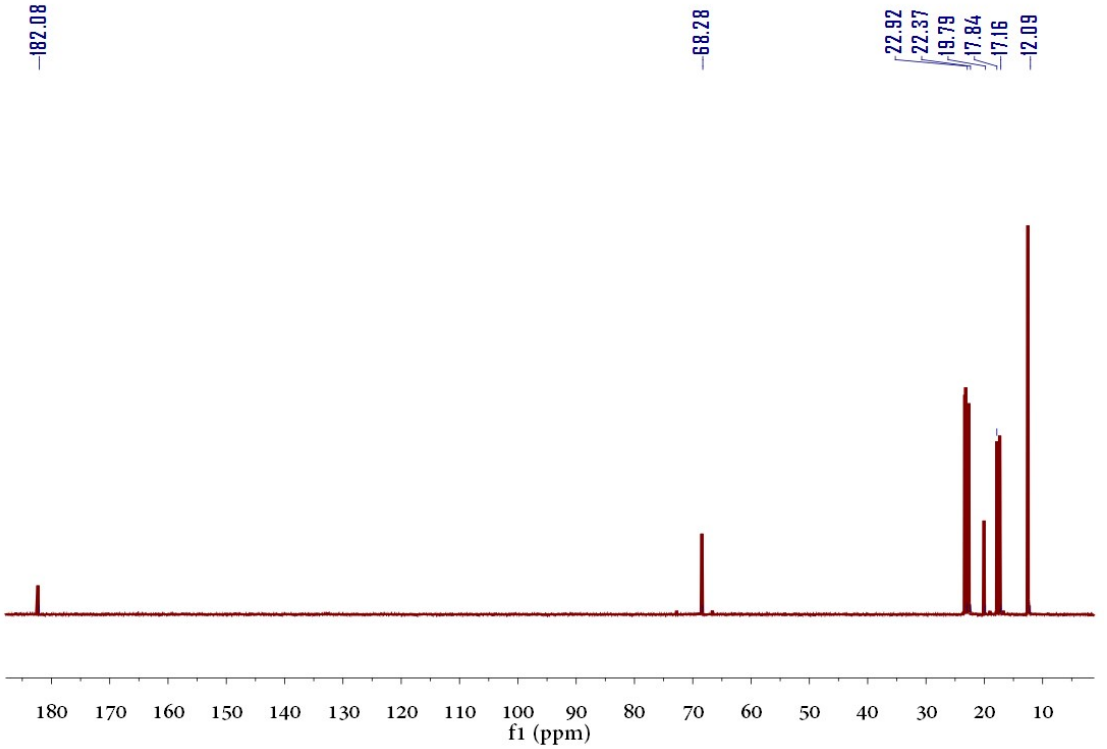

Fig. S9 The ^{13}C NMR spectrum of $[P_{4444}][LAc]$ (D_2O).

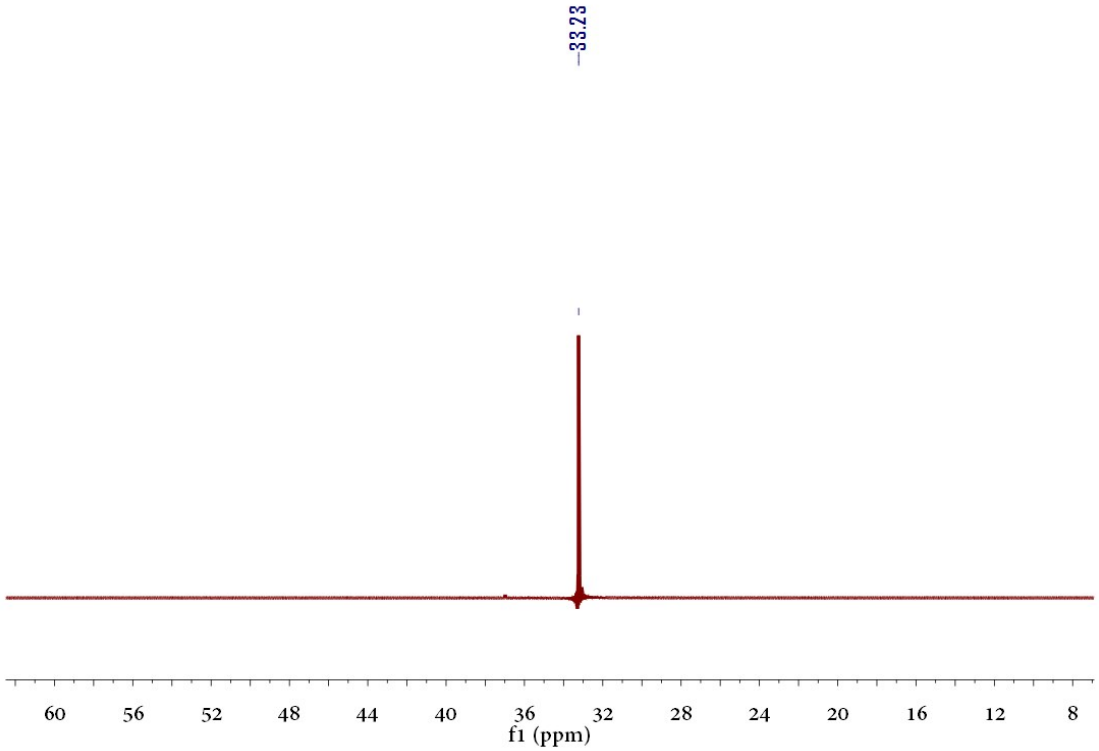

Fig. S10 The ^{31}P NMR spectrum of $[P_{4444}][LAc]$ (D_2O).

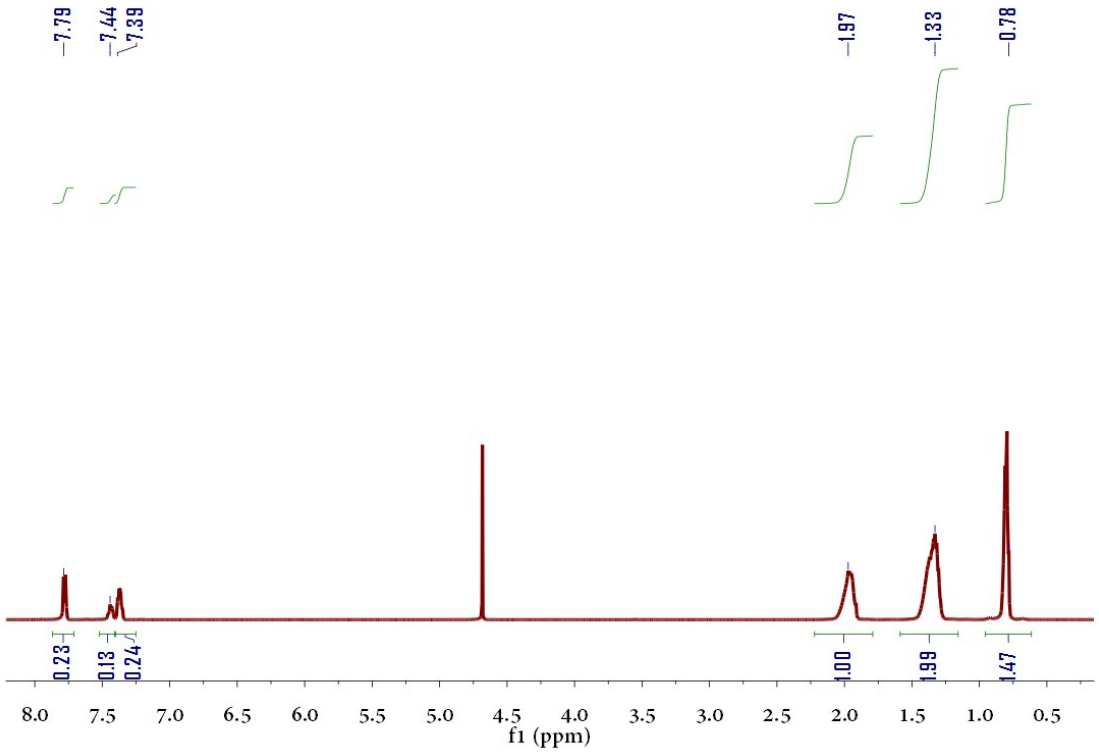

Fig. S11 The ^{1}H NMR spectrum of $[P_{4444}][BAc]$ (D_2O).

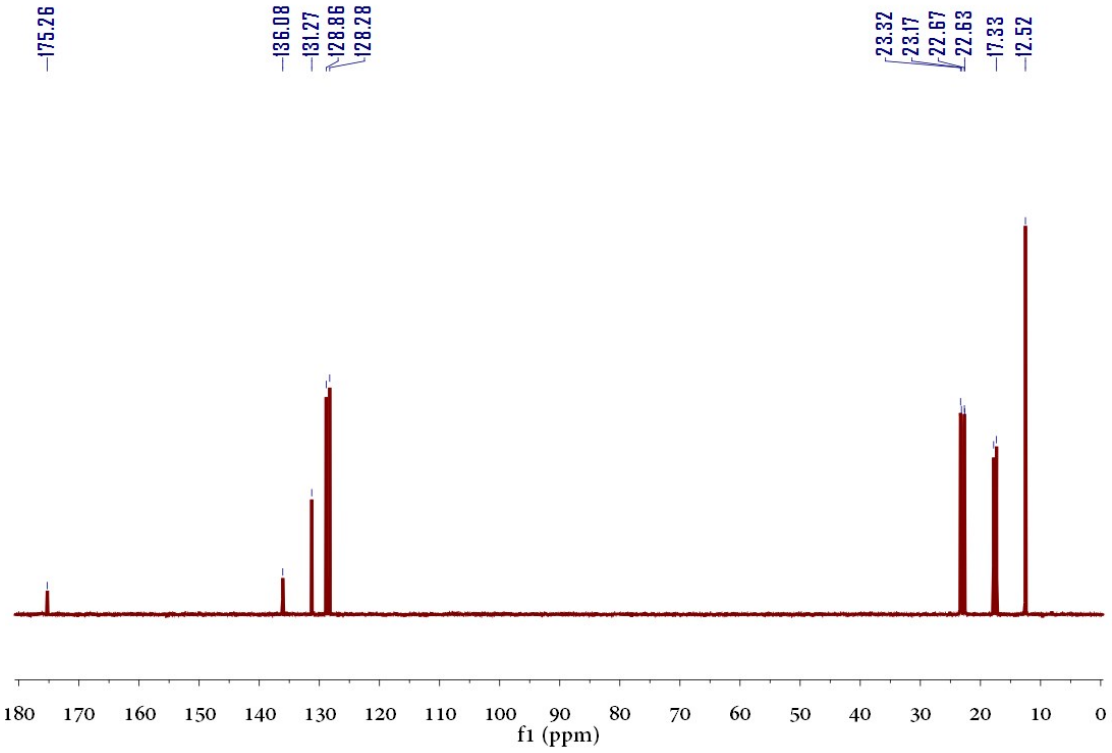

Fig. S12 The ^{13}C NMR spectrum of $[P_{4444}][BAc]$ (D_2O).

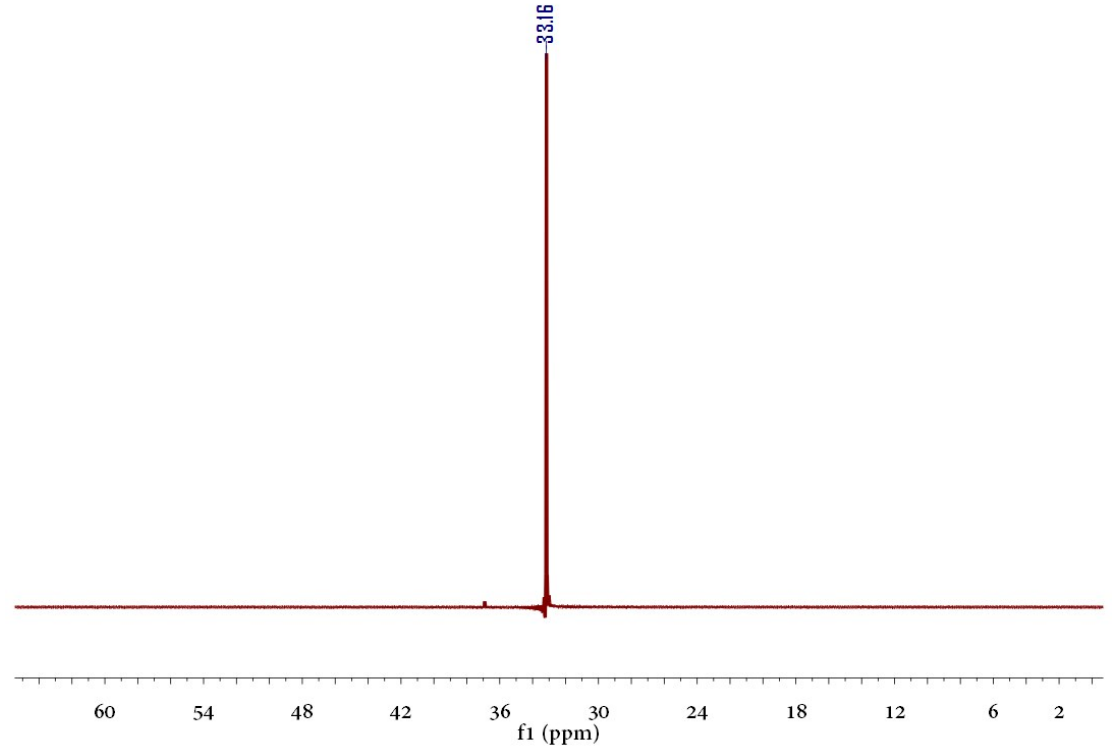

Fig. S13 The ^{31}P NMR spectrum of $[P_{4444}][BAc]$ (D_2O)

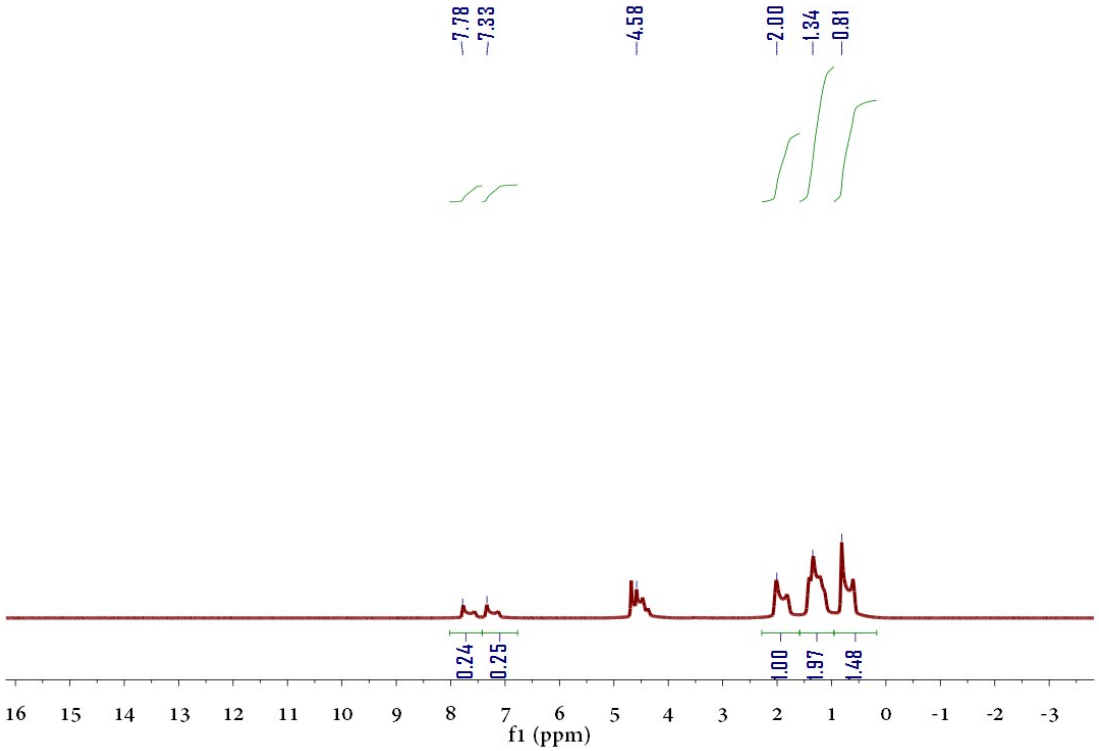

Fig. S14 The ^{1}H NMR spectrum of $[P_{4444}][HMBAc]$ (D_2O)

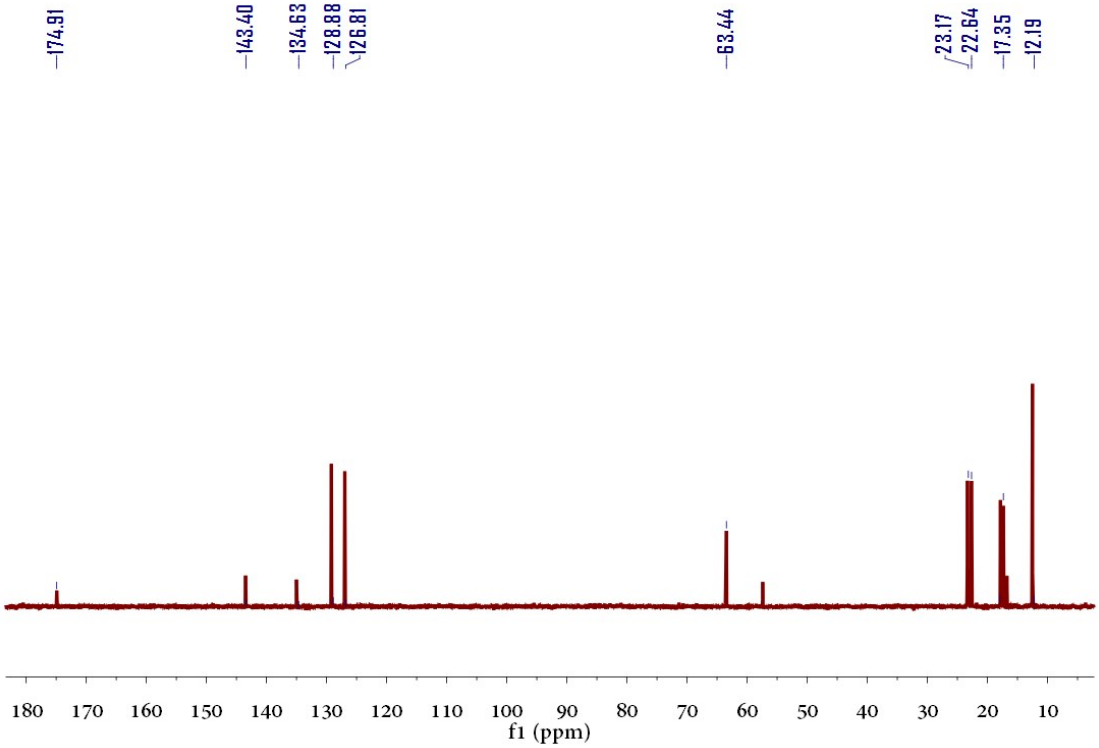

Fig. S15 The ^{12}C NMR spectrum of $[P_{4444}][HMBAc]$ (D_2O)

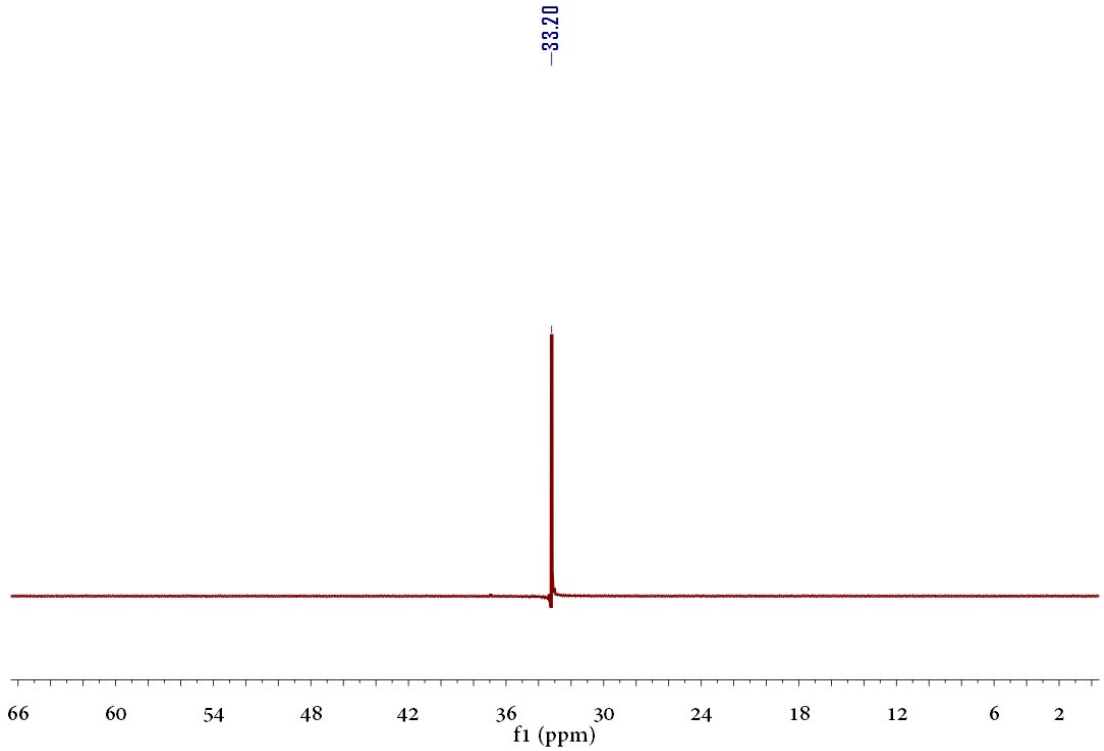

Fig. S16 The ^{31}P NMR spectrum of $[P_{4444}][HMBAc]$ (D_2O)

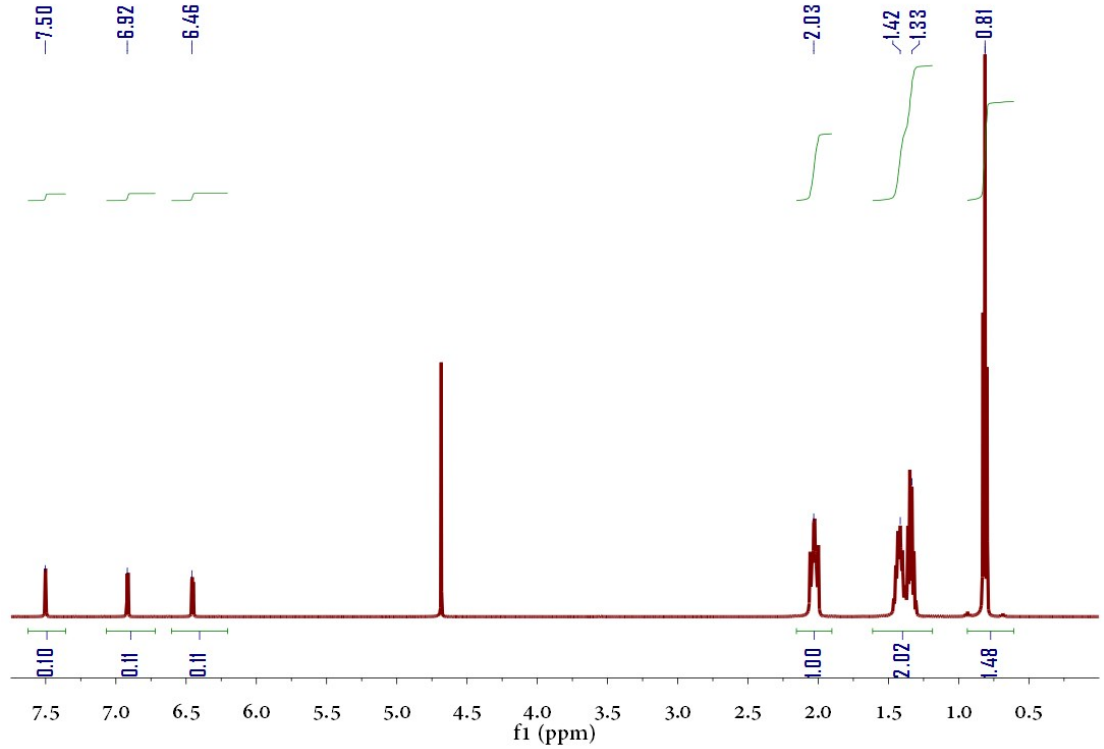

Fig. S17 The ^{1}H NMR spectrum of $[P_{4444}][FAc]$ (D_2O)

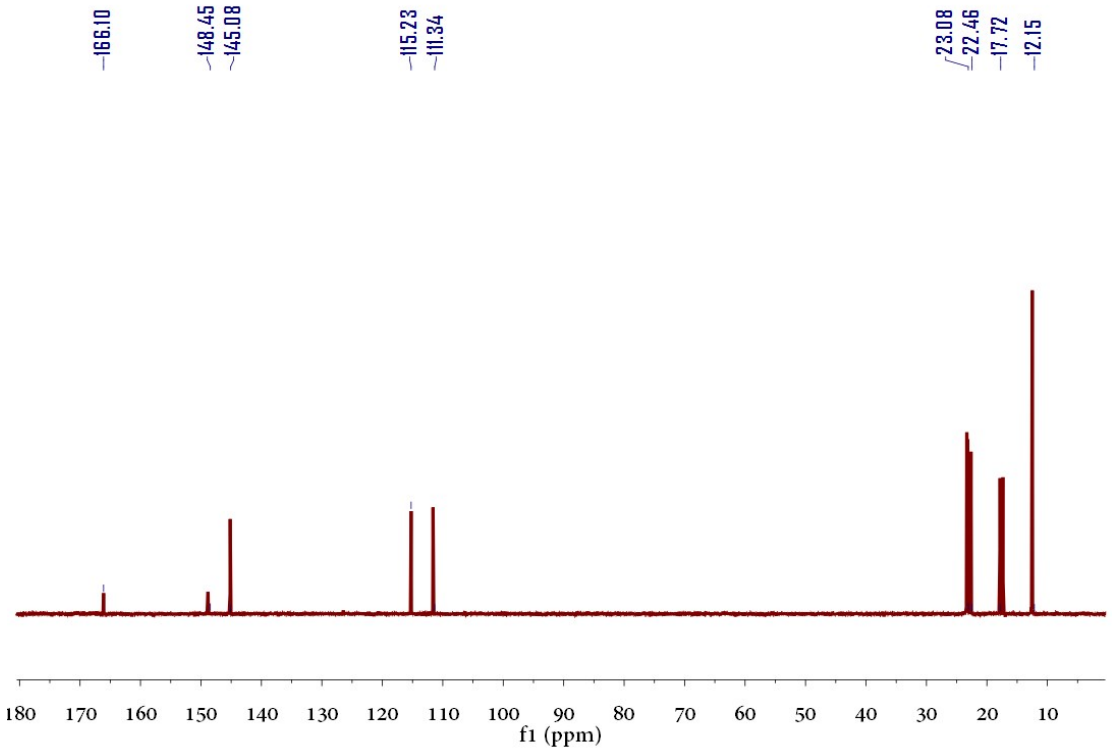

Fig. S18 The ^{13}C NMR spectrum of $[P_{4444}][FAc]$ (D_2O)

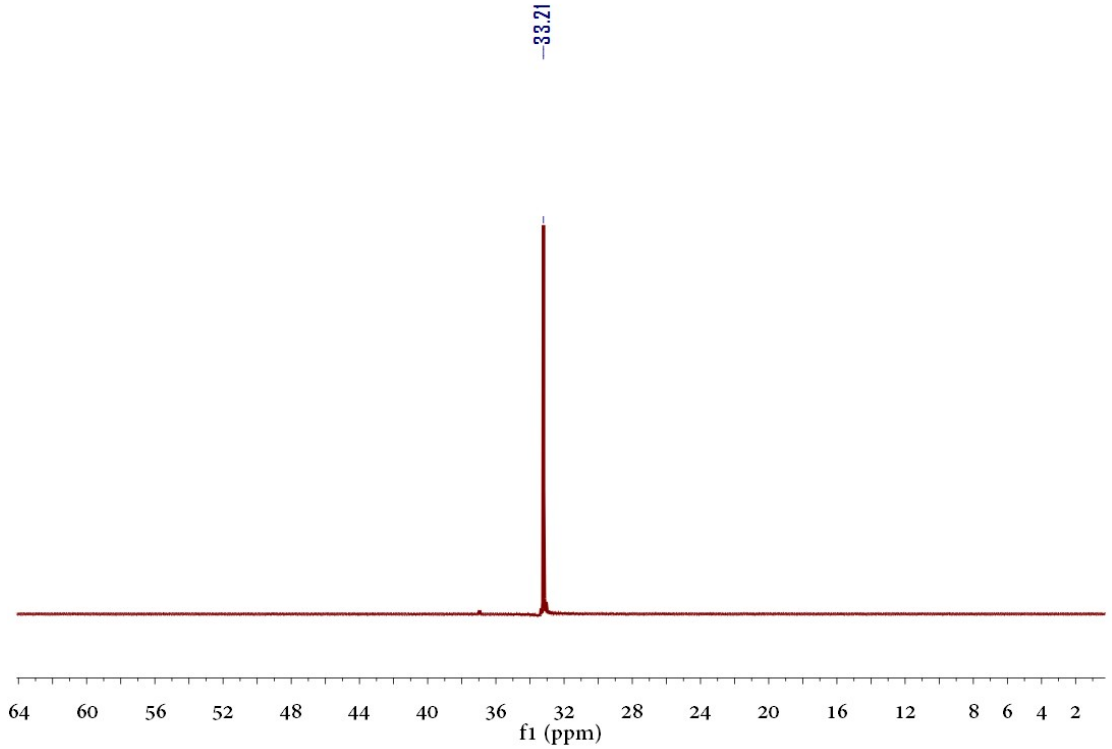

Fig. S19 The ^{31}P NMR spectrum of $[P_{4444}][FAc]$ (D_2O).

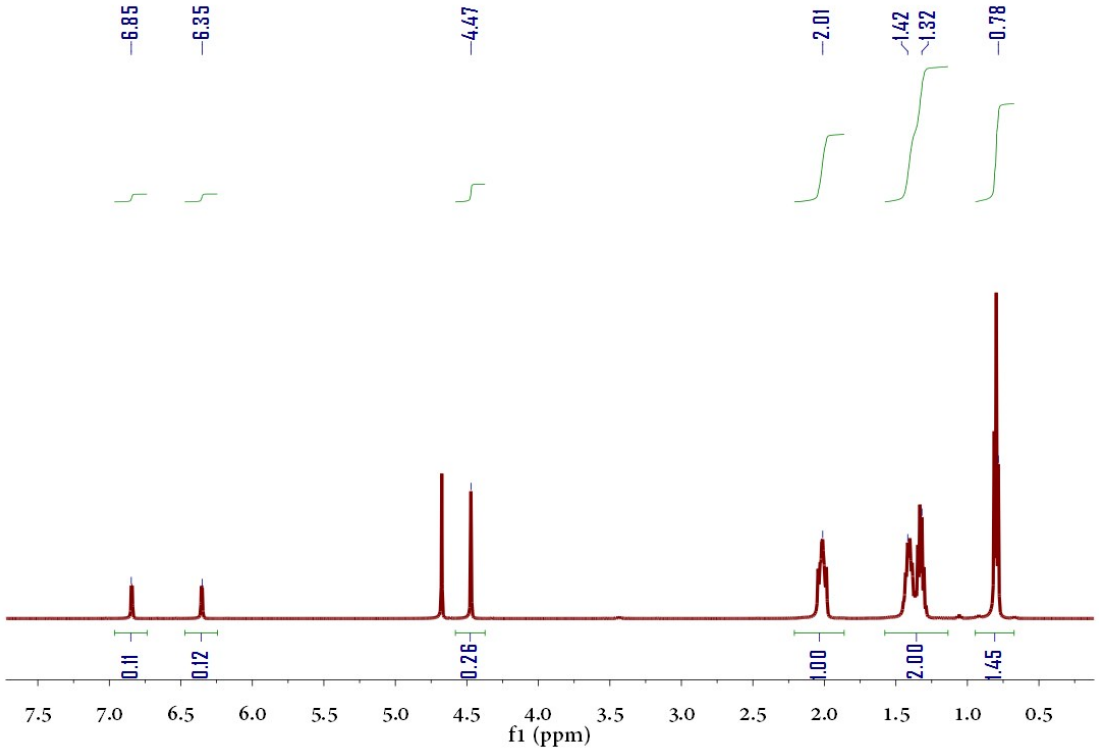

Fig. S20 The ^{1}H NMR spectrum of $[P_{4444}][HMFAc]$ (D_2O)

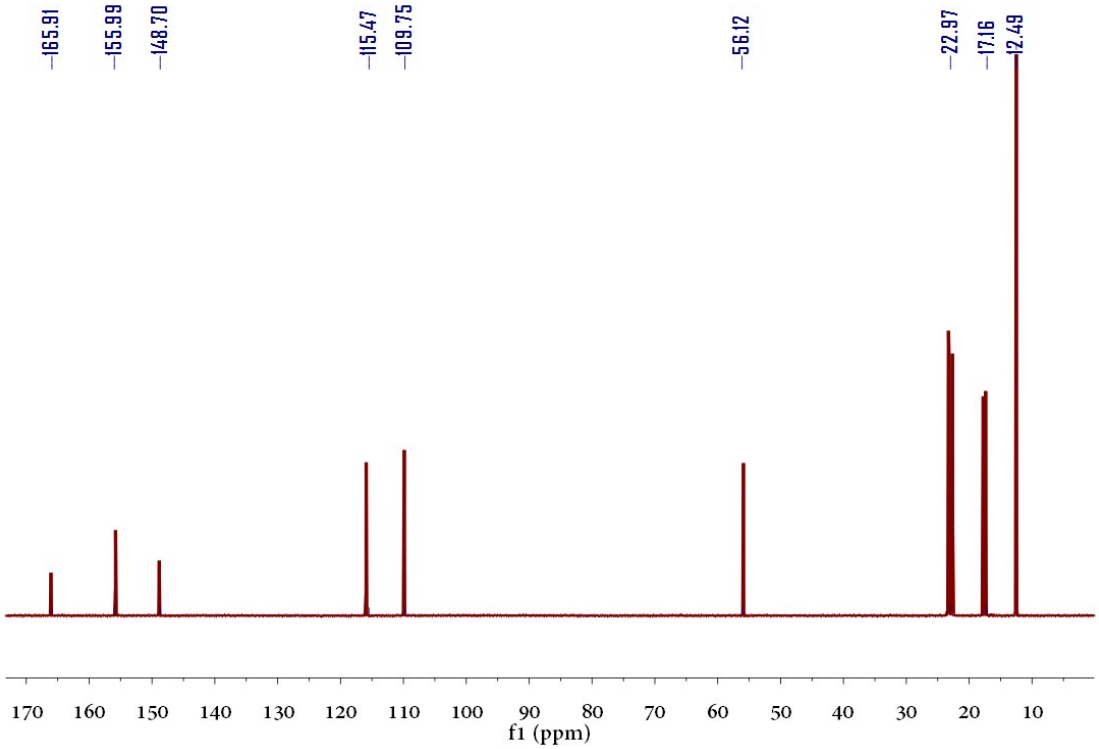

Fig. S21 The ^{13}C NMR spectrum of $[P_{4444}][HMFAc]$ (D_2O)

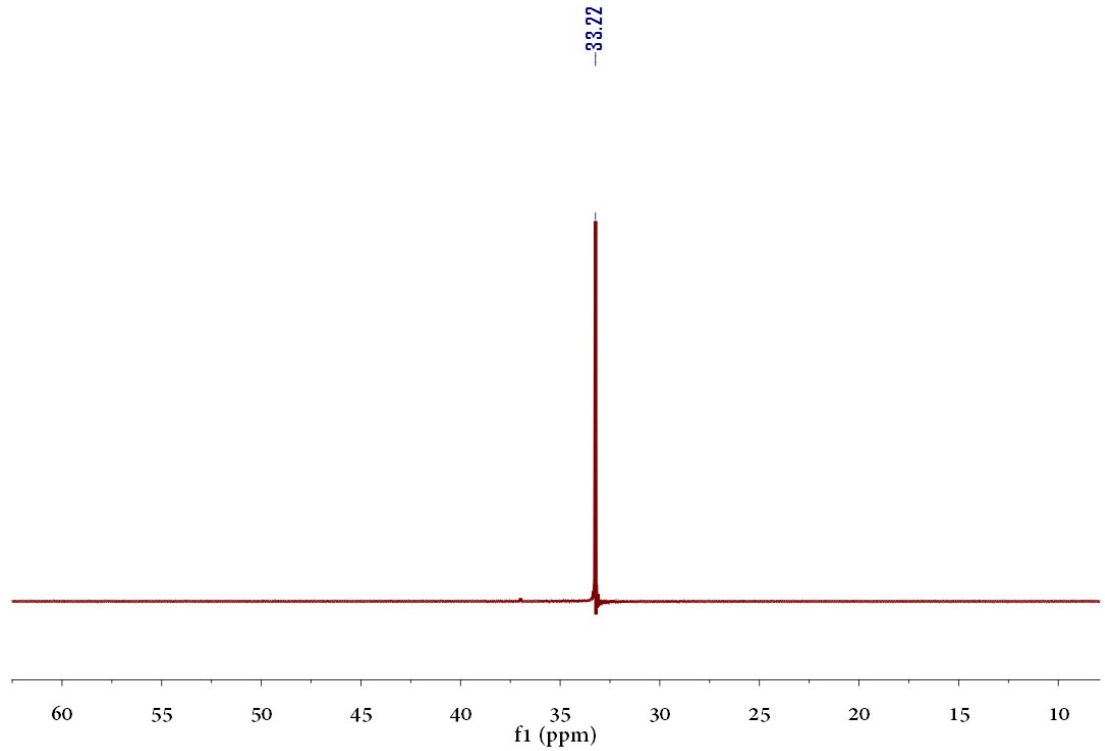

Fig. S22 The ^{31}P NMR spectrum of $[P_{4444}][HMFAc]$ (D_2O)

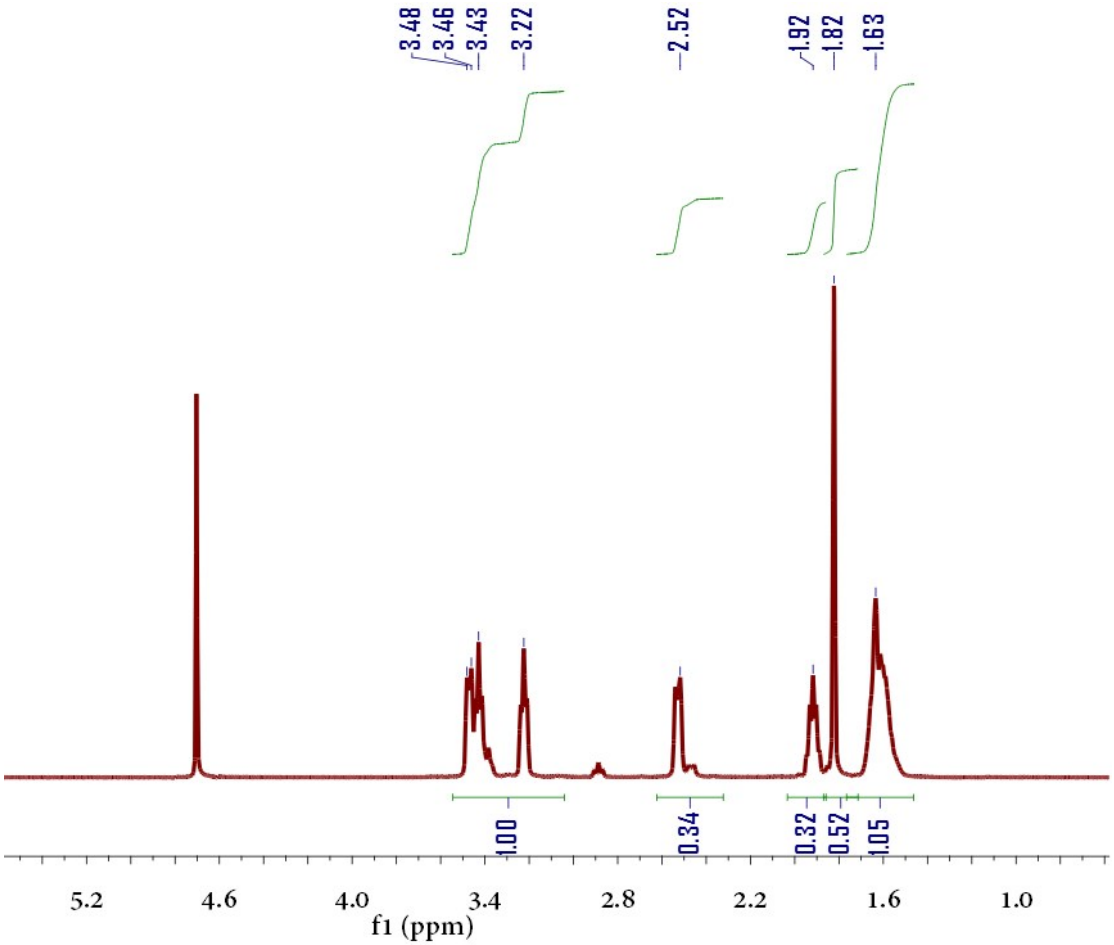

Fig. S23 The ^{1}H NMR spectrum of [DBU][OAc] (D_2O)

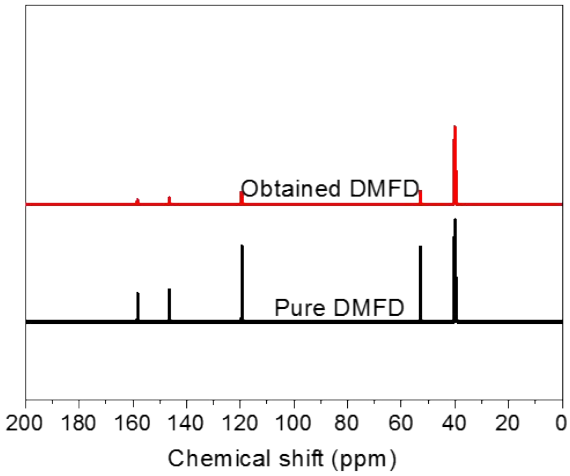

Fig. S24 ^{13}C NMR patterns of the obtained DMFD and the pure DMFD

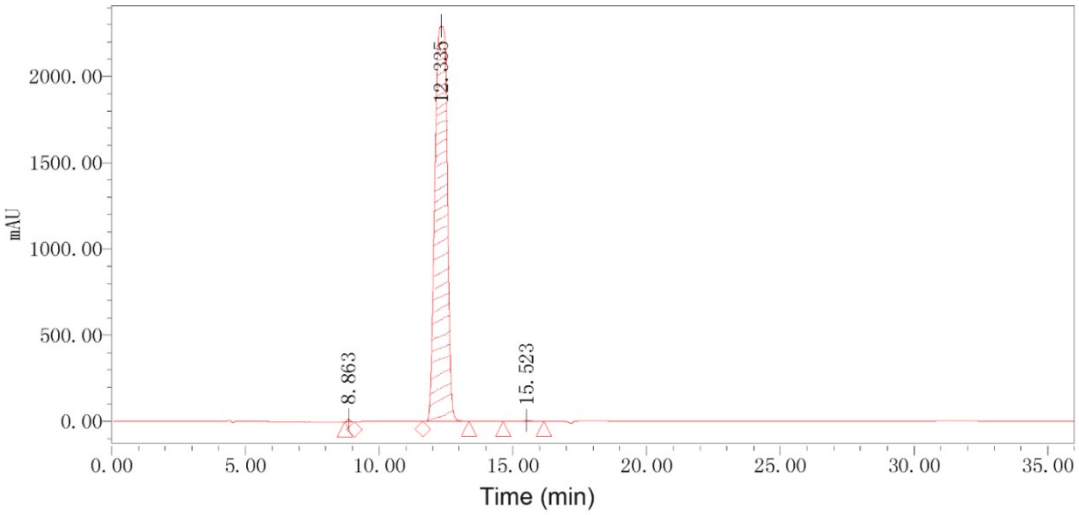

Fig. S25 HPLC spectrum of the obtained DMFD.

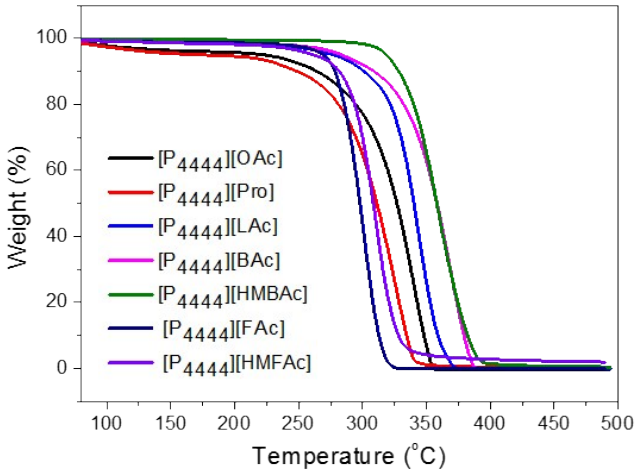

Fig. S26 TGA curves of tetrabutylphosphonium-based ILs

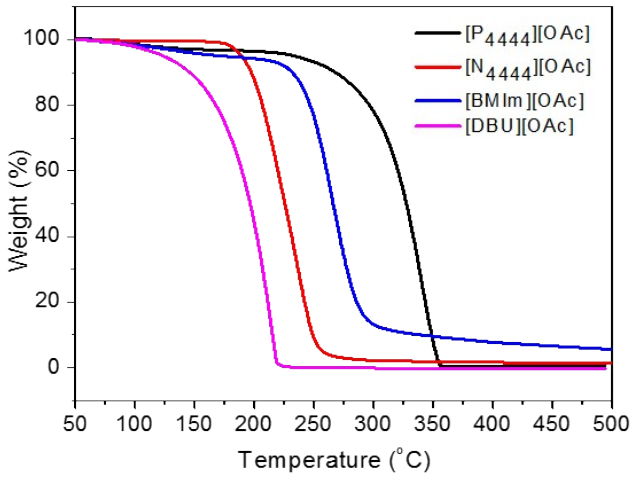

Fig. S27 TGA curves of acetate ILs.

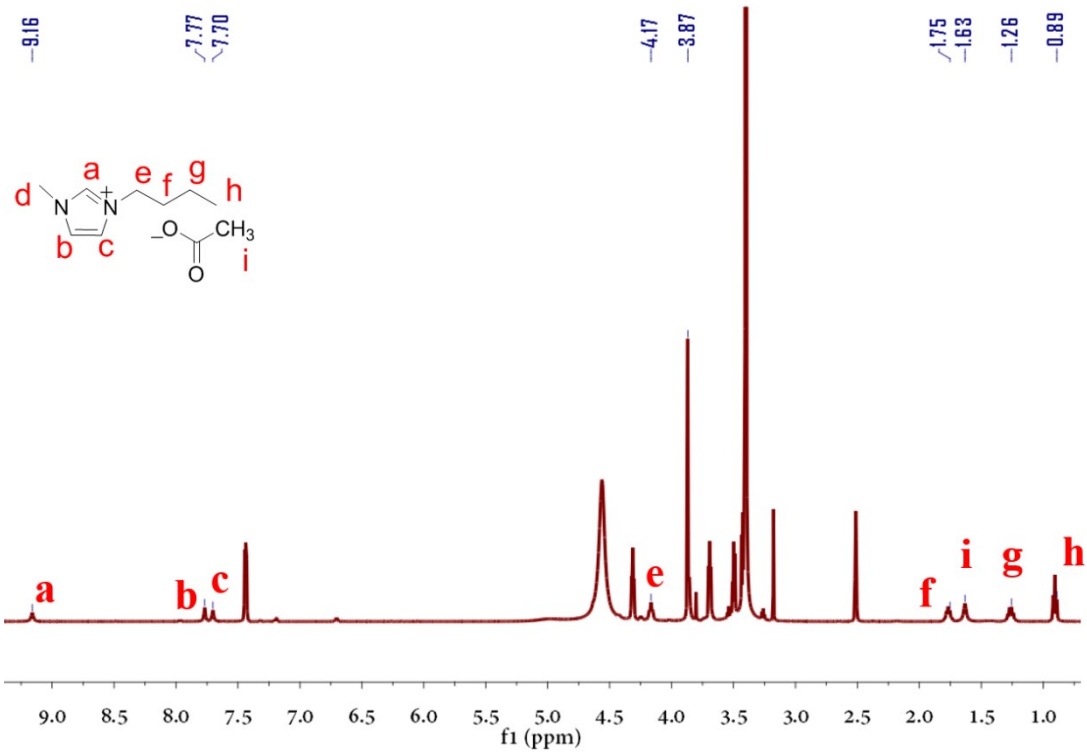

Fig. S28 ^{1}H NMR pattern of [BMIM][OAc] in the filtrate.

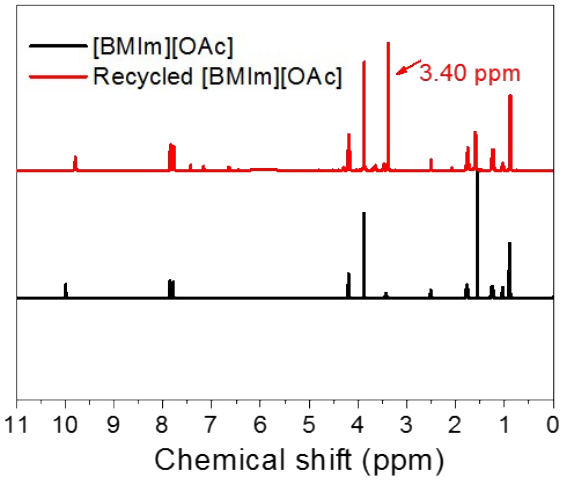

Fig. S29 ^{1}H NMR patterns of recycled [BMIM][OAc] and pristine [BMIm][OAc].

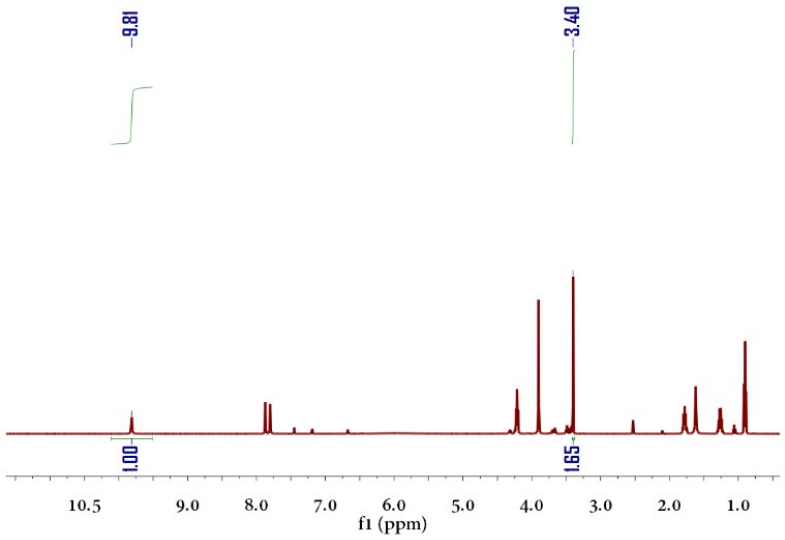

Fig. S30 ^{1}H NMR pattern of recycled [BMIM][OAc].

Theoretical Method

The computations were carried out by using the Gaussian 16 program (Revision B01).[1] The theoretical method was the popular DFT-B3LYP[2-4] adding the D3 version of Grimme's dispersion with Becke-Johnson damping damping function.[5] The triple zeta turbomole basis set, Def2-TZVP, was used for the C, H, N, O atoms[6].

References

[1] M. J. Frisch, G. W. Trucks, H. B. Schlegel, G. E. Scuseria, M. A. Robb, J. R. Cheeseman, G. Scalmani, V. Barone, G. A. Petersson, H. Nakatsuji, X. Li, M. Caricato, A. V. Marenich, J. Bloino, B. G. Janesko, R. Gomperts, B. Mennucci, H. P. Hratchian, J. V. Ortiz, A. F. Izmaylov, J. L. Sonnenberg, D. Williams-Young, F. Ding, F. Lipparini, F. Egidi, J. Goings, B. Peng, A. Petrone, T. Henderson, D. Ranasinghe, V. G. Zakrzewski, J. Gao, N. Rega, G. Zheng, W. Liang, M. Hada, M. Ehara, K. Toyota,

R. Fukuda, J. Hasegawa, M. Ishida, T. Nakajima, Y. Honda, O. Kitao, H. Nakai, T. Vreven, K. Throssell, J. A. Montgomery, Jr., J. E. Peralta, F. Ogliaro, M. J. Bearpark, J. J. Heyd, E. N. Brothers, K. N. Kudin, V. N. Staroverov, T. A. Keith, R. Kobayashi, J. Normand, K. Raghavachari, A. P. Rendell, J. C. Burant, S. S. Iyengar, J. Tomasi, M. Cossi, J. M. Millam, M. Klene, C. Adamo, R. Cammi, J. W. Ochterski, R. L. Martin, K. Morokuma, O. Farkas, J. B. Foresman, and D. J. Fox, Gaussian 16, Revision B.01, Gaussian, Inc., Wallingford CT, 2016.

[2] D. Becke, Density-functional exchange-energy approximation with correct asymptotic-behavior. Phys. Rev. A, 1988, 38, 3098-3100.

[3] A. D. Becke, Density-functional thermochemistry. III. The role of exact exchange. J. Chem. Phys., 1993, 98, 5648-5652.

[4] C. Lee, W. Yang, R. G. Parr, Development of the Colle-Salvetti correlation-energy formula into a functional of the electron density. Phys. Rev. B, 1988, 37, 785-789.

[5] S. Grimme, S. Ehrlich, L. Goerigk, Effect of the damping function in dispersion corrected density functional theory. J. Comput. Chem., 2011, 32, 1456-1465.

[6] F. Weigend, R. Ahlrichs. Balanced basis sets of split valence, triple zeta valence and quadruple zeta valence quality for H to Rn: Design and assessment of accuracy. Phys. Chem. Chem. Phys., 2005, 7, 3297-3305.